IOPscience iopscience.iop.org

Home Search Collections Journals About Contact us My IOPscience

Magnetism and origin of non-monotonous concentration dependence of the bulk modulus in Fe-rich alloys with Si, Ge and Sn: a first-principles study

This article has been downloaded from IOPscience. Please scroll down to see the full text article.

2006 J. Phys.: Condens. Matter 18 6677

(http://iopscience.iop.org/0953-8984/18/29/009)

View the table of contents for this issue, or go to the journal homepage for more

Download details:
IP Address: 129.252.86.83
The article was downloaded on 28/05/2010 at 12:22

Please note that terms and conditions apply.

INSTITUTE OF PHYSICS PUBLISHING JOURNAL OF PHYSICS: CONDENSED MATTER

J. Phys.: Condens. Matter **18** (2006) 6677–6689 doi:10.1088/0953-8984/18/29/009

Magnetism and origin of non-monotonous concentration dependence of the bulk modulus in Fe-rich alloys with Si, Ge and Sn: a first-principles study

T Khmelevska[1], S Khmelevskyi[1,3], A V Ruban[2] and P Mohn[1]

[1] Center for Computational Materials Science, Vienna University of Technology, Getreidemarkt 9/134, A-1060 Vienna, Austria
[2] Applied Material Physics, Department of Materials Science and Engineering, Royal Institute of Technology, SE-100 44 Stockholm, Sweden

E-mail: sk@cms.tuwien.ac.at

Received 5 April 2006, in final form 8 June 2006
Published 30 June 2006
Online at stacks.iop.org/JPhysCM/18/6677

Abstract

Using the first-principles calculations based on the coherent potential approximation, we study the electronic structure, magnetic moments and the bulk modulus of FeX alloys with IVB group elements (X = Si, Ge, Sn) in the Fe-rich concentration range (x = 0.0–0.25), which form a stability region of bcc-related phases. In agreement with experiment, our calculations reproduce well a peculiar non-monotonous behaviour of the bulk modulus in Fe–Si alloys with increasing Si concentration. Such a dependence is found for all bcc-related disordered and partially ordered Fe–Si phases A2, B2 and $D0_3$, which is in contrast with an earlier suggestion that the non-monotonous bulk modulus behaviour is related to partial ordering in Fe–Si. In addition, our results predict a similar behaviour in Fe–Ge and Fe–Sn alloys. It is shown that the observed behaviour of the bulk modulus is entirely related to the changes of the magnetic properties with chemical composition.

1. Introduction

The crystalline Fe–Si alloys with low Si concentrations are widely used magnetic materials [1]. These materials have a number of interesting properties related to the complex interplay between the chemical order and magnetism of the Fe—both being extremely sensitive to the composition and details of the sample preparation (e.g. heat treatment) [1–3]. The phase diagram in the concentration range 0–25 at.% of Si includes three bcc-based structures, A2, B2 and $D0_3$, and shows a tendency to phase sequence A2–B2–$D0_3$ with increasing Si content

[3] Author to whom any correspondence should be addressed.

 © 2006 IOP Publishing Ltd Printed in the UK

but with significant regions of phase coexistence [4]. The phases can be considered to result from different kinds of chemical ordering on a bcc lattice: A2 (α-Fe), B2 (CsCl type), and $D0_3$ ($AlFe_3$ type). The exact phase boundaries, however, largely depend on the conditions of sample preparation [2].

As Si is doped into pure Fe, the spontaneous magnetization gradually decreases [1]. Fallot [5] noted that, for small Si concentrations, this decrease is approximately proportional to the concentration of Si atoms. However, as the Si concentration increases, Mössbauer studies [6, 7] revealed the presence of Fe atoms with different magnetic moments, suggesting a strong dependence of the Fe moments on the local atomic environment. Substitution of Si also leads to a large decrease in the magnetic anisotropy and makes Fe–Si steels very soft magnetic material with huge prospects for electrical energy saving applications (see [1, 8] and references therein).

The magnetic properties and their dependence on the Si content were the subject of numerous theoretical models, starting from Neel's hypothesis [9] about oriented ordering of the Si atoms in Fe–Si, which only recently seems to have been confirmed experimentally [3], and phenomenological models by Niculescu *et al* [10] and Elsukov *et al* [11]. These models rely mainly on assumptions relating the Fe moments to the local chemical environment.

Iron-rich Fe–Si materials have been studied intensively during the past two decades using first-principles electronic structure calculations. Most attention has been paid, however, to ordered Fe_3Si. The first *ab initio* studies of magnetism in this compound were performed by Williams *et al* [12] who calculated the values of magnetic moments of Fe on different crystallographic sites in the $D0_3$ lattice. A recent thorough investigation, including mechanical and elastic properties, based on full potential density functional theory band structure methods, was presented by Moroni *et al* [13], where also references on other relevant studies can be found (see also the first-principles study of magnetism under pressure in Fe_3Si in [14]).

Despite the fact that the knowledge of the calculated electronic structure and site distribution of magnetic moments in ordered Fe_3Si can be useful to draw some rough qualitative conclusions about the physical situation in disordered Fe–Si alloys with lower Si content, more insight can be provided only by calculating the electronic structure for realistic disordered alloys in the actual chemical composition. Moreover, as will be shown in this paper, the concentration dependence of some properties, like the bulk modulus of Fe–Si alloys in the range between 0 and 25 at.% Si, cannot be considered just as an interpolation between highly diluted Fe–Si alloys and the Fe_3Si compound. With full-potential density functional theory based methods, one can model some particular alloy compositions by using large artificial ordered supercells and calculate, for example, the distribution of the moments on the various Fe sites with different local atomic environments. Arzhnikov and Dobysheva [15] have applied this method for ordered $Fe_{15}Si$ and $Fe_{15}Sn$ alloys and found a considerable dependence of atomic Fe magnetic moments on the distance to the silicon *impurity*. However, it is hard to progress with this approach to the study of the concentration dependence of various alloy properties, especially if they also depend strongly on the degree of chemical ordering. Apart from technical difficulties—to model various possible atomic configurations, large supercells are required—there is also a fundamental problem connected to the fact that many important observed properties of disordered alloys, e.g. magnetization or mechanical properties, are averages over all possible atomic configurations.

A conventional approach to calculate such configurationally averaged alloy properties from first principles is to use the coherent potential approximation (CPA) [16]. The application of CPA within the framework of the local spin density approximation (LSDA) to disordered Fe–Si alloys with $D0_3$ symmetry by Kudrnovský *et al* [17] provided a microscopic basis for earlier phenomenological descriptions [10] of the Fe moments and their concentration dependence.

Kulikov *et al* [18], using the CPA, studied substantially disordered bcc (A2-structure) $Fe_{1-x}Si_x$ alloys in the range $0 < x < 0.25$. For this particular Fe–Si phase, apart from magnetic properties, the concentration dependences of the equilibrium volume and the bulk modulus were also determined. They found that much better agreement with experimental values can be achieved with the use of the general gradient approximation (GGA) to the exchange and correlation potential compared to LSDA.

In section 3 we present the results of our first-principles CPA study of the phases (A2, B2, $D0_3$) of Fe–Si alloys. We provide a detailed comparison of their magnetic properties, lattice constants and bulk moduli in the whole range of chemical compositions between pure Fe and ordered Fe_3Si. Moreover, we have included in our study the iron-rich alloys with other IVB group elements, namely Fe–Ge and Fe–Sn. The physical properties of these alloys have been much less studied experimentally. This is because of their limited solubility range with pure Fe (only up to ∼10 at.% for Ge and Sn [4]) and their less attractive technological prospects. Consequently, much less theoretical attention was paid to them too; for instance, no first-principles studies of disordered Fe–Sn and Fe–Ge have been reported so far. However, quite recently, progress in mechanical alloying has allowed the preparation and investigation of the magnetic properties of stable and metastable Fe–Sn solid solutions in a wide range of chemical compositions [19]. This was done in particular for the disordered bcc structure that exists up to 32 at.% Sn. In section 4 the physical origin of the peculiar concentration dependence of the bulk modulus in Fe–Si alloys is discussed.

The problem of the non-monotonous behaviour the of bulk modulus of Fe–Si was originally pointed out by Kulikov *et al* [18] who, analysing the experimental data of various authors on elastic constants of Fe–Si alloys, noted that the bulk modulus exhibits a minimum in the concentration range 0–25 at.% Si.

In this paper we will argue that the bulk modulus anomaly is *entirely* related to the magnetism of the alloys considered. Namely, it is a result of an additional magnetic softening of the bulk modulus, which is strongly concentration dependent and arises from the Fe magnetic moment dependence on the crystal volume. We believe that our results will contribute to the general discussion about the complex interplay between magnetism and structural properties in Fe–Si alloys, which is indeed a crucial issue for applications [1].

2. Calculational details

The electronic structure of Fe–X alloys (X = Si, Sn, Ge) has been calculated using the *ab initio* Korringa–Kohn–Rostoker (KKR) method in the atomic-sphere approximation (ASA), as described in [23, 24]. The partial waves in the KKR-ASA calculations have been expanded up to $l_{\max} = 3$ inside the atomic spheres. All calculations were performed within the scalar relativistic approximation, which contains all relativistic effects with the exception of spin–orbit coupling.

In contrast to previous KKR studies of the A2 Fe–Si phase [18], in all our calculations the total energy was calculated using multipole screening electrostatic corrections (up to $l = 6$) to the electrostatic potential and energy [25], which significantly improves the accuracy of the ASA results [23, 26]. Substitutional chemical disorder in Fe–X alloys was treated using the coherent potential approximation (CPA). In the case of partially ordered B2 or $D0_3$ structures of Fe–Si, the unit cell contains two or three non-equivalent sites respectively, but only one of them becomes partially populated by Si.

For an accurate description of the equilibrium volumes and bulk moduli of transition metals within the framework of the local spin-density approximation (LSDA), one needs to employ the general gradient approximations (GGA) [27]. The importance of the GGA, in particular

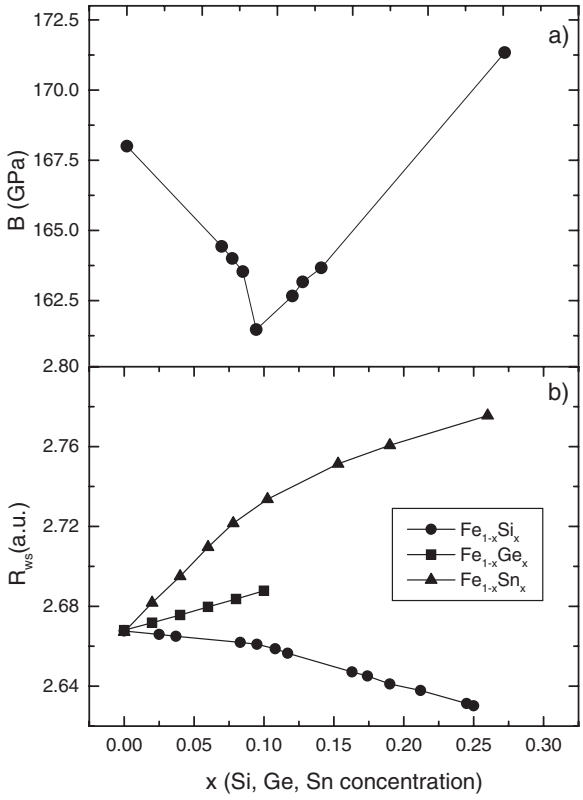

Figure 1. Experimental bulk modulus (extracted from [20, 21], as described in the text) and lattice constants [4, 19] of $Fe_{1-x}Si_x$, $Fe_{1-x}Ge_x$ and $Fe_{1-x}Sn_x$.

for Fe–Si, has been discussed in detail in [18]. In agreement with [18], we also find that pure LSDA [28] strongly underestimates the equilibrium lattice constants (by about 3%) and correspondingly overestimates the bulk modulus compared to experiment. For pure Fe, our LSDA results for the equilibrium Wigner–Seitz atomic radius is 2.54 and 2.62 au with GGA, which should be compared to an experimental value of 2.67 au. Much better agreement with experiment using GGA was also reported from full-potential studies of ordered Fe_3Si [13]. This motivated us to only present results from calculations based on the GGA local exchange and correlation potential [27].

All calculations presented were converged on a uniform mesh of $29\times29\times29$ k-points in the full cubic (B2), bcc (A2) and fcc ($D0_3$) Brillouin zone (BZ). The convergence of the results was checked by increasing the number of k-points for the BZ integration up to $41\times41\times41$ k-points for some particular cases. The achieved stability of the results is better than 0.01 mRyd/atom for the total energy, 10^{-4} au for the lattice constants, and 1% for the calculated bulk moduli.

3. Magnetism and bulk modulus in Fe–Si, Fe–Ge and Fe–Sn alloys

Before we present our results, we recall the experimental findings. In figure 1 (upper panel) we show this non-monotonous behaviour of the bulk modulus B, as calculated from the experimental elastic constants $B = \frac{1}{3}(c_{11} + 2c_{21})$ given in [20, 21]. Since their GGA calculations of the bulk modulus for the disordered A2 phase failed to reproduce the minimum

in B, the authors of [18] suggested that it may only appear as a result of increasing ordering in Fe–Si alloys with increasing Si content. As we will show later, the GGA-based calculations reproduce the experimental concentration behaviour well for the A2 phase too. Moreover, we find a similar behaviour for the B2 and $D0_3$ ordered phases. Our calculations also predict that such a minimum also appears for Fe–Sn and Fe–Ge alloys, only shifted to lower Sn/Ge concentrations. This behaviour of the bulk modulus is particularly interesting, since simple chemical bonding arguments based on a phenomenological tight-binding model would suggest a monotonous decrease in the bulk modulus with increasing p-element concentration. This behaviour is due to the increasing number of p–d and p–p bonds, which are much more rigid than corresponding highly *metallic* d-bonds in pure Fe (see, e.g., chapter 8.1 in [22]). The changes in the lattice constants (unit cell volumes) caused by the substitutions give no clear hint to this non-monotonous behaviour. In the lower panel of figure 1 we collected data on the experimental concentration dependence of the lattice constants for the Fe–X (X = Si, Sn, Ge) alloys plotted as a function of the average Wigner–Seitz atomic radius R_{WS}. The respective curves are fairly monotonous and the slopes have a different sign for Fe–Si and Fe–Sn/Ge, whereas a bulk modulus anomaly is found for all of them.

Here we present a comparative study of the three phases of Fe–Si alloys with 0–25 at.% Si and with different Si ordering on the underlying bcc lattice, namely A2, B2 and $D0_3$. It will be shown that differences in the properties of these phases are mainly determined by distinct magnetic properties of Fe on the different sublattices. An interesting observation can already be made by comparing the calculated equilibrium atomic Wigner–Seitz radii R_{WS} presented in the upper panel of figure 2. They are related to the lattice constant a of the underlying body centred cubic lattice according to $a = (16\pi/3)^{1/3} R_{\mathrm{WS}}$. One notes that, compared to the fully disordered A2 phase, the lattice constant in the partially ordered phases decreases much faster with increasing Si concentration. Moreover, although the lattice constant of the A2 phase also decreases, the rate of the changes is only negligibly smaller if compared to experiment [4], so that this decrease may be viewed as a consequence of the ordering in realistic samples. We emphasize this point here because: (i) for the discussion of the experimental results (see, e.g., [3]) it is sometimes assumed that Si has a smaller atomic radius than Fe and that this in some way may explain a reduction in the moments of Fe atoms neighbouring the Si sites; (ii) earlier first-principles CPA studies of Fe–Si were performed either without lattice constant optimization [17] or they considered only the A2 phase [18]. Indeed, pure Si with a diamond structure and, more relevant in this context, hypothetical metallic bcc Si (see [29] and the results presented in the next section) both have an atomic volume larger than pure bcc Fe. The decreasing lattice constant in Fe–Si alloys upon adding Si is a consequence of the decreasing Fe magnetic moment and not vice versa. The calculated reduction in the average moment per Fe for all three phases is shown in the lower panel of figure 2. This effect is much larger for the ordered phases, which explains the difference in the concentration dependence of R_{WS} shown in the upper panel. In addition, we note that the magnetic moment decreases with increasing Si content also if one chooses the lattice constant to be fixed for all chemical compositions, e.g. equal to those of pure Fe or Fe_3Si. We do not show the results for fixed R_{WS}, but for the $D0_3$ phase they can be found in [17].

Calculating the equilibrium R_{WS} (figure 1) using GGA yields good agreement with the experimental values, but slightly underestimates them by $\sim$1.5%. This is the reason for a concomitant overestimation of the calculated bulk moduli B (middle panel of figure 2) compared to experiment. However, they are well within the range of the usual LSDA/GGA error bar (20–30%) [30]. The important point is that the intrinsic error of the spin-density approximation depends not so much on the alloy composition. As a result, the observed experimental concentration dependence of the bulk moduli are well reproduced in

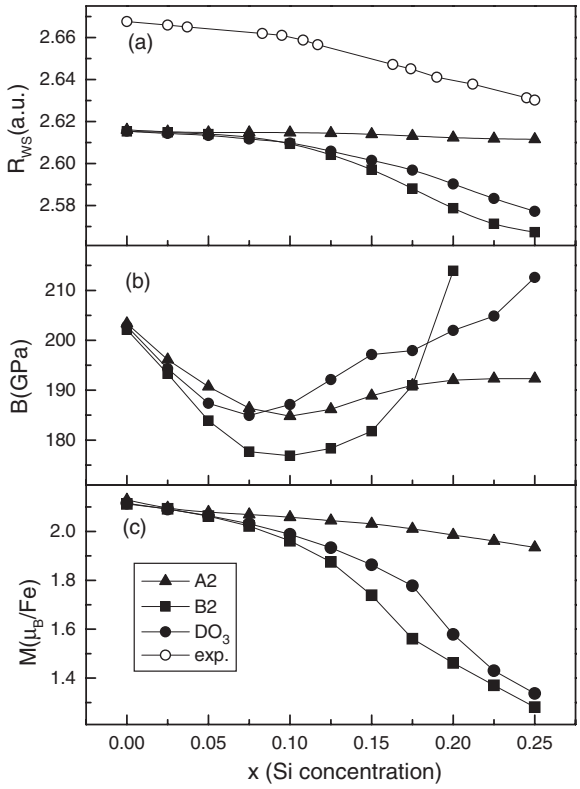

Figure 2. Calculated ground-state properties: (a) atomic Wigner–Seitz radii; (b) bulk moduli; and (c) average atomic Fe moments for three phases of $Fe_{1-x}Si_x$—A2, B2 and $D0_3$.

the calculations for all three Fe–Si phases. It thus appears that the minima in the concentration dependence of the bulk modulus is an intrinsic property of the Fe–Si alloys and is not related to the changes of the chemical order with higher Si content. From figure 2 it can be seen that, in the range of 0–7 at.% Si, the bulk modulus B decreases with Si alloying independently of the degree of chemical order. For all three samples, the respective curves turn downwards, whereas in the region of higher concentrations, where only the $D0_3$ structure can be stabilized [4], it should increase again. Since the absolute value of B for the present alloys depends on ordering, the exact form of $B(x)$ would also depend on the details of the sample preparation. It can be seen from figure 2 that the lattice constants, as well as the average magnetic moments, monotonously decrease providing no hints for any non-monotonous behaviour of B. The suggestion given in [18] that this is related to the changes in the structural ordering are also not confirmed by our analysis. A discussion of the origin of this peculiar behaviour is given in section 4.

In figure 3 we plot the calculated moments of the Fe atoms on non-equivalent lattice sites of Fe–Si alloys with B2 and $D0_3$ partial ordering. Fe(I) denotes Fe atoms on Si sublattices of B2, Fe(II) are atoms that are neighbours to Si; and Fe(III) are on the sublattice of the $D0_3$ structure with no Si atoms in the nearest coordination shell. The moments of Fe(II) atoms in both B2 and $D0_3$, which have Si neighbours, drop rapidly with increasing Si composition, which provides a justification for the assumptions made in the phenomenological theories given in [3, 10]. In contrast, the moments of the iron atoms on the Si sublattice, Fe(I), and also on the Fe(III) sites of $D0_3$, gradually increase. This increase explains, in particular, why the calculated

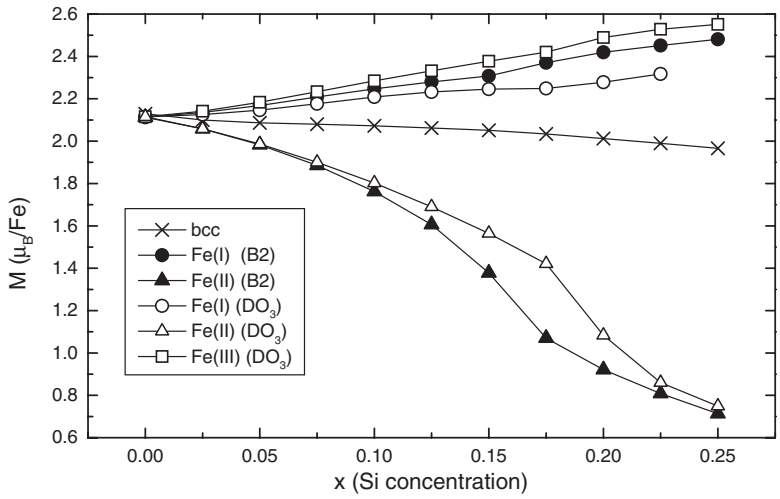

Figure 3. Atomic magnetic moments on Fe non-equivalent sites in A2, B2 and $D0_3$ phases of $Fe_{1-x}Si_x$. For details of notation, see text.

moments of Fe(II) in $D0_3$ Fe–Si alloys [17] are lower than estimated phenomenologically [10] by assuming that the moments on Fe(I) and Fe(III) sites remain constant with a value as in pure bcc Fe. Our results for the $D0_3$ structure show that the Fe(II) moments depend non-linearly on the Si concentration x, in contrast to the results given in [17]. This is due to the fact that we also consider changes in the lattice constant upon Si alloying, which leads to an additional decrease of the moments, whereas the calculations reported in [17] used the same lattice constant for all alloy compositions. The observed large decrease in the moments on the Fe(II) sites is in good agreement with previous full-potential results for the $D0_3$ ordered Fe_3Si intermetallic compound [13]. The Fe moments on the individual sublattices change monotonously for all three structures, as do the lattice constants and the average moments (figure 2). The difference in the concentration dependence of the lattice constant between the fully disordered A2 structure and the partially ordered structures is related to the rapid decrease in the moment on the Fe(II) sublattice.

The fact that the moment of Fe atoms that are nearest neighbours of Si is strongly reduced compared to its value in pure bcc Fe is a central issue for the successful interpretation of many experimental results, in particular for the technologically important Fe–Si alloys with B2-type ordering [3]. However, based on our results for the B2 structure, we note that there is no reason to explain this strong reduction as a consequence of the local inter-atomic distance variation [3]. It appears to be a purely chemical effect caused by the participation of the iron d-electrons in the formation of p–d bonds, well reproduced in the calculations without any assumptions on the local inter-atomic distance changes. The induced moment on Si is very small, $\sim$0.01 μ_B for all concentrations, and has the opposite direction to the Fe moments.

Let us now turn to Fe–Sn and Fe–Ge cubic alloys, which have the same number of valence electrons as Fe–Si. Compared to Fe–Si, they show a more limited range of solubility and, up to now, no pronounced technological importance. However, they deserve attention, since recent studies of metastable Fe–Sn in a wide range of concentrations [19] revealed some interesting trends in their magnetic behaviour, different from Fe–Si. In particular, the magnetization measurements [19] suggested that the average magnetic Fe moment in Fe–Sn increases up to $\sim$5 at.% Sn and then turns out to be more or less constant up to 25 at.% Sn. In

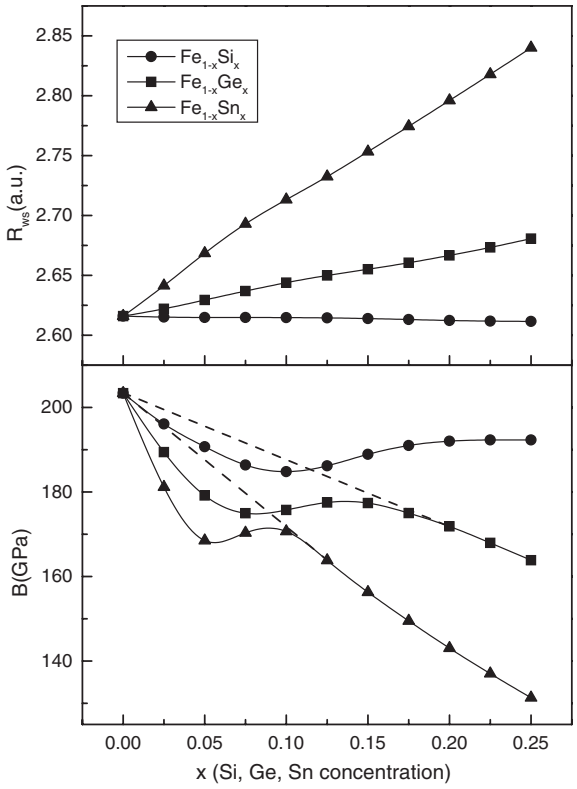

Figure 4. Calculated ground-state atomic Wigner–Seitz radii (upper panel) and bulk moduli (lower panel) of fully substitutionally disordered phase (A2) of $Fe_{1-x}Si_x$, $Fe_{1-x}Ge_x$ and $Fe_{1-x}Sn_x$ alloys.

addition, a comparison of their calculated properties with those of Fe–Si will be rather useful for the understanding of the peculiar concentration behaviour of the bulk modulus. To our best knowledge, there exist no reports on the ordering tendencies in Fe–Sn and Fe–Ge, so that we study only the fully disordered A2 phase.

The calculated ground state R_{WS} and bulk moduli of Fe–Sn and Fe–Ge are shown in figure 4, where the corresponding values for the A2 phase of Fe–Si are also given. One can conclude from the upper panel that the experimental trend concerning the lattice constant behaviour (compare to figure 1) is readily reproduced for all three alloys. In contrast to Fe–Si, the lattice constants of Fe–Ge and Fe–Sn increase upon p-element doping, however the bulk moduli show the same peculiar behaviour (lower panel). The position of the minimum of the bulk modulus is just shifted to lower concentrations of the p-element. The average Fe moment also behaves differently than in Fe–Si. For Fe–Sn alloys, it sharply rises for small concentrations and then only gradually increases. This is in good agreement with experimental results (see figure 10 in [19]). The reason for the initial sharp increase in the Fe moment upon Sn doping is the large expansion of the lattice caused by the p-element, however as more Sn is doped, the formation of a larger number of p–d bonds tends to reduce the Fe moment, similarly to the Fe–Si case. The competition of the two effects is nicely illustrated in the Fe–Ge case (figure 5), where the moment gradually grows for low Ge concentration and then even decreases.

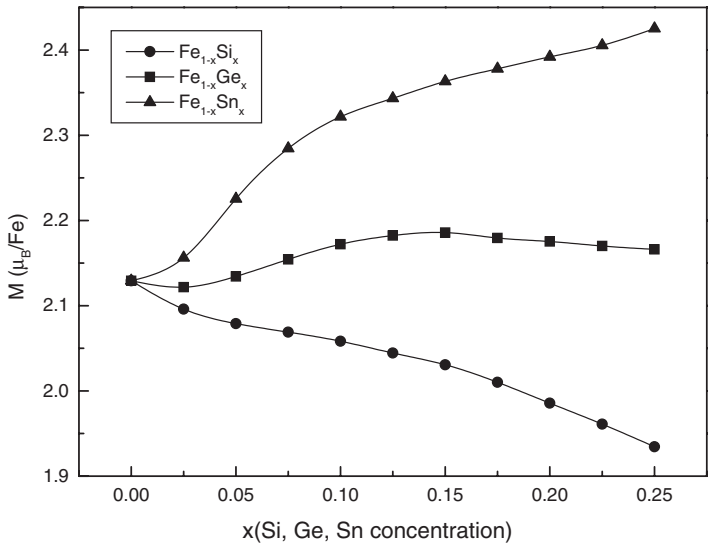

Figure 5. Calculated Fe atomic moments of $Fe_{1-x}Si_x$, $Fe_{1-x}Ge_x$ and $Fe_{1-x}Sn_x$ alloys in A2 phase.

The curves shown in the lower panel of figure 4 also gives a hint concerning the origin of the peculiar bulk modulus behaviour in these alloys, which can hardly be explained by considering Fe–Si alone. Starting from a certain concentration (∼15 at.% Ge and ∼10 at.% Sn), the bulk modulus shows a monotonous decrease, as one would expect from the simple tight-binding arguments given in the introduction (increasing number of rigid p–d and p–p bonds). If we continue this monotonous curve down to zero concentration (the dotted lines in figure 4), one realizes that one needs to explain the source of some additional negative contributions to the bulk modulus, which has a maximum at a peculiar concentration of the p-element and then tends to vanish for higher concentrations.

4. Dependence of bulk modulus on the p-element concentration

Since the concentration dependence of the bulk modulus shows a minimum for all three phases of Fe–Si, we concentrate on the A2 phase. For the A2 phases of Fe–Sn and Fe–Ge alloys, we noted that the minimum of the $B(x)$ dependence can be considered as a result of some negative contribution, which depends on the alloy concentration. In order to see whether this is also true for Fe–Si alloys, we extend our calculations of the A2 phase beyond the range of stability of the bcc phase. In the upper panel of figure 6, the calculated equilibrium R_{WS} and B are shown for the full range 0–100 at.% Si. It can be seen that the lattice constant of the A2 Fe–Si phase indeed increases compared to pure bcc Fe. Starting from about 25 at.% Si, the bulk modulus indeed monotonously decreases, as is expected from the general arguments about chemical bonding given above. If one now extrapolates this monotonous behaviour to low Si concentration (dotted curve), we have a similar picture as in the A2 phases of Fe–Sn and Fe–Ge (figure 4).

In the lower panel of figure 6, we present results from a non-spin-polarized (non-magnetic) calculation of the A2 phase of Fe–Si alloy. The equilibrium volumes of these artificial non-magnetic alloys are, as expected, much smaller than for the corresponding magnetic alloys

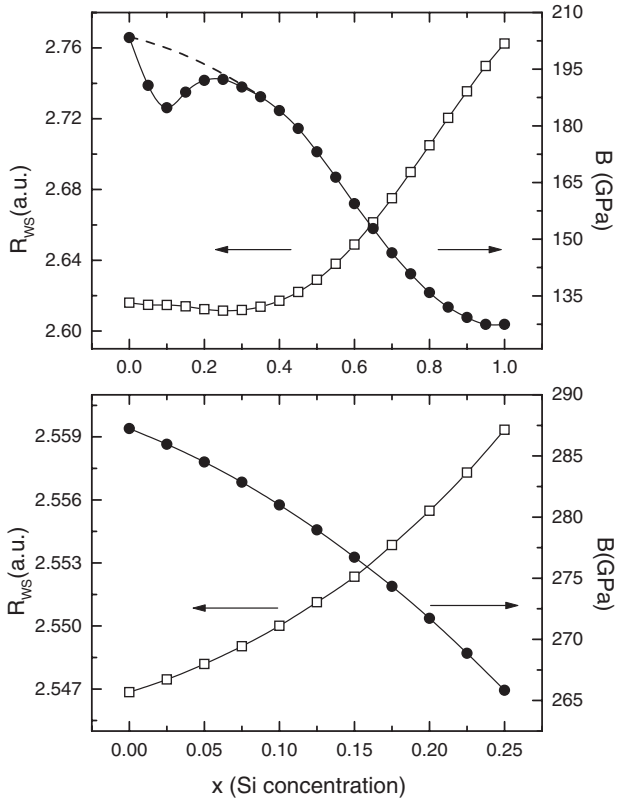

Figure 6. Calculated ground-state atomic Wigner–Seitz radii and bulk moduli of $Fe_{1-x}Si_x$ alloys (A2 phase) for: (1) upper panel, in full range of concentrations; (2) lower panel, for a hypothetical non-magnetic (non-spin-polarized) state.

and monotonously increase with Si concentration. It can be seen that the non-magnetic bulk modulus does not show any anomaly in its concentration dependence, decreasing monotonously in the whole range of alloy compositions. One can therefore deduce that the origin of the bulk modulus anomaly is entirely magnetic.

In the previous section we have seen, however, that the changes of the average magnetic moments (as well as on individual Fe sites, in the case of B2 and $D0_3$ phases) are monotonous. This suggests that one needs to look at the derivatives of the magneto-volume characteristics. Since we only deal with the $T = 0$ K ground state, we can apply a simple mean-field picture of itinerant magnetism, in which, to lowest order, the total energy E depends on the magnetic moment of iron via a term which is proportional to the square of magnetization M^2 [22]:

$$E(M) = E_0 - IM^2 + \cdots$$

whered I is some positive constant (usually called the Stoner exchange parameter), which is a mainly intra-atomic property of the magnetic element, depending only weakly on the alloy composition. From the definition of the bulk modulus

$$B = V_0(\partial^2 E/\partial V^2)_{V=V_0},$$

where V_0 is the equilibrium volume. After taking the derivatives, the magnetic contribution to the bulk modulus consists of two terms. It is easy to see that one of them is proportional to the

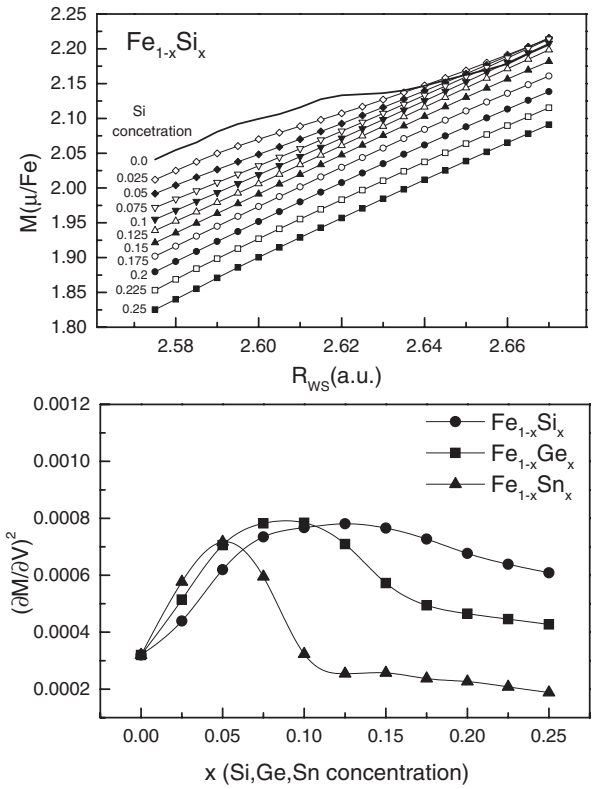

Figure 7. Upper panel: calculated dependence of the average Fe moment on the average Wigner–Seitz radii of the bcc lattice for various $Fe_{1-x}Si_x$ alloy compositions. Lower panel: square of the derivative of the magnetic moment per unit cell with respect to the unit cell volume at the equilibrium lattice constants (see text for details).

square of the derivative of M with respect to the volume:

$$B_{\mathrm{m}} = -V_0 I (\partial M/\partial V)^2_{V=V_0}. \tag{1}$$

Since the moment normally increases monotonously with the volume, the magnetic contribution (1) is in general negative and leads to a softening of the bulk modulus, which is of major interest for the following discussion.

The second term is proportional to the second derivative of the moment with respect to the volume. This contribution is much smaller than the first term, because the curvature of the moment/volume dependence (see upper panel of figure 7) is almost negligible over the whole volume range. In the upper panel of figure 7, we show the calculated dependence of the Fe moment on R_{WS} for various concentrations of Si in the A2 phase. It can be seen that curves are not parallel, in particular for small Si concentrations, where they even intersect at larger volumes. At the same time, for larger Si concentration, the curves become less steep. Since all curves increase monotonically with volume, the contribution B_{m} from (1) is negative for all compositions. To estimate its order of magnitude, we numerically calculate the derivative of the squared magnetization per atom (which at $T = 0$ K is just the moment per unit cell) with respect to the unit cell volume for the disordered alloys Fe–Si, Fe–Sn and Fe–Ge. The results, in units of $(\mu_{\mathrm{B}}/\mathrm{au})^2$, are presented in the lower panel of figure 7. The maximum of the derivatives in all three alloys, i.e. the maximum of the respective negative contribution to B, are

found to occur at the same concentrations where the corresponding minima of B appear in the calculations (see also figure 4). One thus can conclude that the behaviour of the bulk modulus is entirely due to the non-monotonous changes of the moment/volume derivative as a function of the concentration. We thus could show that the minimum in the concentration dependence of the bulk modulus is due to a magnetic softening effect whose value strongly depends on the p-element concentration.

5. Conclusions

We presented a comparative first-principles study of the magnetic and elastic properties of three stable phases of $Fe_{1-x}Si_x$ and the related fully disordered $Fe_{1-x}Sn_x$ and $Fe_{1-x}Ge_x$ alloys in the concentration range $x = 0$–0.25. We found that the experimentally observed moderate decrease in the Fe–Si lattice constant upon Si alloying in the considered concentration range is a consequence of a chemical ordering tendency rather than just the 'smaller' Si ionic radius. In the partially ordered B2 and $D0_3$ structures, the decrease in the lattice constant is a consequence of the decreasing Fe moments on nearest-neighbour sites of the Si sublattice, therefore being a magnetic effect, which is in contrast to some earlier interpretations of the magnetic moment changes due to local lattice contraction effects. Applying first-principles CPA, we study the partially ordered B2 structure in the whole range of chemical composition, and found that the magnetic moment on the Fe sublattice nearest to Si decreases even faster than in the corresponding $D0_3$ case studied earlier.

Despite a monotonous change of the lattice constant and the magnetic moments upon the concentration of the p-element, we calculate the respective non-monotonous bulk modulus dependence, which is in accordance with available experimental data on Fe–Si alloys. The reason for the minimum in the bulk modulus versus p-element concentration curve is shown to be due to a negative magnetic contribution leading to an additional softening of B. This contribution is related to changes in the derivative of the magnetic moment with respect to the volume and has the same origin as those leading to the bulk modulus softening in Invar alloys.

Since there exist almost no experimental data on the elastic properties of the bcc-related phases of Fe–Sn and Fe–Ge alloys and on their dependence on chemical order in Fe–Si alloys, we hope that the results of this study will motivate future experimental work in this direction.

References

[1] Bertotti G, Ferchmin A R, Fiorillo E, Fukamichi K, Kobe K and Roth S 1994 Magnetic alloys for technical applications *Soft Magnetic Alloys, Invar and Elinvar Alloys* (*Landolt Börnstein New Series* vol III/19i1) (Berlin: Springer) pp 33–143
[2] Nilfrish K, Kolker W, Petry W and Scharpf O 1994 *Acta Metall. Mater.* **42** 743
[3] Chernenkov Yu P, Fedorov V I, Lukshina V A, Sokolov B K and Ershov N V 2003 *J. Magn. Magn. Mater.* **254/255** 346
[4] Predel B 1995 *Phase Equilibria, Crystallograpic and Thermodynamic Data of Binary Alloys* (*Landolt Börnstein New Series* vol IV/5 sub H) ed O Madelung (Berlin: Springer)
[5] Fallot M 1936 *Ann. Phys., Lpz.* **6** 305
[6] Stearns B M 1963 *Phys. Rev.* **129** 1136
[7] Stearns B M 1971 *Phys. Rev.* B **4** 4069
[8] Shim J S, Bae J S, Kim H J, Lee H M, Lee T D, Lavernia E J and Lee Z H 2005 *Mater. Sci. Eng.* A **407** 282
[9] Neel L 1951 *J. Phys. Rad.* **12** 339
[10] Niculescu V A, Burch T J and Budnik J I 1983 *J. Magn. Magn. Mater.* **39** 223
Niculescu V A, Raj H, Budnick I J, Hines W A and Menotti A H 1976 *Phys. Rev.* B **14** 4160
[11] Elsukov E P, Konygin G N, Barinov V A and Voronina E V 1992 *J. Phys.: Condens. Matter* **4** 7597
[12] Williams A R, Moruzzi A T, Gelatt C D Jr, Kübler J and Schwarz K 1982 *J. Appl. Phys.* **52** 2019

[13] Moroni E G, Wolf W, Hafner J and Podloucky R 1999 *Phys. Rev.* B **59** 12860
[14] Rhee J Y and Harmon B N 2004 *Phys. Rev.* B **70** 094411
[15] Arzhnikov A K and Dobysheva L V 2000 *Phys. Rev.* B **62** 5324
[16] Turek I, Drchal V, Kudrnovký J, Šob and Weinberger P 1997 *Electronic Structure of Disordered Alloys, Surfaces and Interfaces* (Boston: Kluwer–Academic)
[17] Kudrnovký J, Christensen N E and Andersen O K 1991 *Phys. Rev.* B **43** 5924
[18] Kulikov N I, Fristot D, Hugel J and Postnikov A V 2002 *Phys. Rev.* B **66** 014206
[19] Yelsukov E P, Voronina E V, Konygin G N, Barinov V A, Godovikov S K, Dorofeev G A and Zagainov A V 1997 *J. Magn. Magn. Mater.* **166** 334
[20] Machová A and Kadeková A 1977 *Czech J. Phys.* B **27** 555
[21] Kaiser M X and Gibson M D 1966 *ISAEC Rept. IS* **1500** M70
Every A G and McCurdy A K 1991 *Second and Higher Order Elastic Constants* (*Landolt Börnstein New Series* vol III/29/a) (Berlin: Springer) p 31
[22] Pettifor D 1995 *Bonding and Structure of Molecules and Solids* (Oxford: Clarendon)
[23] Ruban A V and Skriver H L 1999 *Comput. Mater. Sci.* **15** 119
[24] Abrikosov I A and Skriver H L 1993 *Phys. Rev.* B **47** 16532
[25] Christensen N E and Satpathy S 1995 *Phys. Rev. Lett.* **55** 600
[26] Ruban A V, Simak S I, Korzhavyi P A and Skriver H L 2002 *Phys. Rev.* B **66** 024202
[27] Wang Y and Perdew J P 1991 *Phys. Rev.* B **44** 13298
Perdew J P, Chevary J A, Vosko S H, Jackson K A, Pederson M R, Singh D J and Fiolhais C 1992 *Phys. Rev.* B **46** 6671
[28] Perdew J P and Wang Y 1992 *Phys. Rev.* B **45** 13244
[29] Yin M T and Cohen M L 1982 *Phys. Rev.* B **26** 5668
[30] Fast L, Wills J M, Johansson B and Eriksson O 1995 *Phys. Rev.* B **51** 17431